INTERNATIONAL JOURNAL OF PRECISION ENGINEERING AND MANUFACTURING Vol. 19, No. 5, pp. 753-759 MAY 2018 / 753

REGULAR PAPER

DOI: 10.1007/s12541-018-0090-3
ISSN 2234-7593 (Print) / 2005-4602 (Online)

Predicting Three-Dimensional Gait Parameters with a Single Camera Video Sequence

Jungbin Lee[1], Cong-Bo Phan[1], and Seungbum Koo[1,#]

1 School of Mechanical Engineering, Chung-Ang University, 84, Heukseok-ro, Dongjak-gu, Seoul, 06974, Republic of Korea
Corresponding Author / E-mail: skoo@cau.ac.kr, TEL: +82-2-820-5876
ORCID: 0000-0002-4843-1083

KEYWORDS: Gait recognition, Segment length, Three-dimensional pose estimation, Video surveillance

Human gait reflects biomedical conditions and thus can potentially be used for identification. With the increasing utility of CCTVs for surveillance, there have been various attempts to recognize persons using gait image sequences from a single camera. We investigated the accuracy of estimating body segment lengths and joint angles during gait calculated from a video sequence using a gait database. We recruited 30 subjects and collected motion capture data during walking and extracted the trajectories of 17 body points. Principal component analysis (PCA) was applied to the collected gait. We implemented full gait cycle-based (FGC) PCA and gait-phase-specific (GPS) PCA. Three-dimensional poses were estimated from gait event frames using FGC-PCA and GPS-PCA. The estimated poses in discrete gait event frames were interpolated to estimate motion during a full gait cycle. The body pose from GPS-PCA was less sensitive to camera angles and smaller errors compared to FGC-PCA. The segment lengths of the upper arm (r=0.79), lower arm (r=0.63), upper leg (r=0.86), and lower leg (r=0.81) were highly correlated with the lengths obtained from the motion capture data. Three-dimensionally reconstructed human motion can reveal personal biometric information and has the potential to be used for human identification.

Manuscript received: November 20, 2017 / Revised: February 4, 2018 / Accepted: February 5, 2018

1. Introduction

Human gait contains biometric features influenced by individual biomedical conditions and history such as weight as well as serious injuries associated with the joints or brain.[1-5] Gait features have long been studied for identification using video surveillance applications such as smart closed-circuit television (CCTV).[6-16]

Recently, criminals were identified based on gait analysis using CCTV evidence. It was confirmed that gait analysis can be useful in forensic investigations.[17] A bank robber was identified by comparing surveillance footage of a crime scene with the image of the suspect. They contended that, according to gait analysis and anthropometric methods, the suspect and perpetrator could have been the same person. In the U.K., a podiatrist analyzed a burglar's peculiar gait obtained from a CCTV and confirmed that there were considerable similarities between the suspect and perpetrator.[18]

Technically, methods to identify a person using gait can be divided into two main groups. The first group involves motion-based methods.[6-13] This method is based on simple features extracted from video spatial-temporal silhouettes of gait motion without considering a basic geometric model. This method is simple, but the results are sensitive to video view angle.

The second group uses geometric human models and predicts joint angles in two-dimensional (2D) space from video data.[14-16] The results of this method also depend on video view angle. Recently, three-dimensional (3D) structure reconstruction from 2D video sequences has been conducted.[9-26] We reconstructed 3D gait using a 3D pose reconstruction algorithm and then extracted gait parameters. This study explicates a method to extract 3D geometric gait features from a video for individual identification.

1) Body segment length prediction: The length of body segments provides important personal biometric information. Body segment lengths were predicted from a video sequence through 3D human pose reconstruction.

2) Gait interpolation: A three-dimensional interpolation method for joint kinematics was developed to reduce the necessity for manual labeling of joint positions in gait event frames and to reconstruct the kinematics for a full gait cycle.

3) Temporal joint angles: In addition to the body segments, joint movement patterns and their ranges during a gait cycle were extracted

as features for identification.

4) Effect of camera angle: Camera angle relative to gait progression line affects the accuracy of 3D human pose predictions. This study proposes a method to improve accuracy even when the camera is at the front or back of a person by using gait phase information.

2. Related Work and Our Approach

It has been proposed to calculate the 2D joint angles of people from a video sequence using stick figure models.[14-16] Joint center points were marked from video frames, and then 2D models and their joint angles were calculated. However, the 2D models presented motion from a specific camera angle. Recently, studies have been conducted to reconstruct a 3D structure from a 2D image. Tomasi and Kanade[27] proposed that 3D scene geometry and camera motion could be inferred from a stream of images.

Using this concept, Ramakrishna et al.[21] decomposed a 3D human pose into three sets: camera parameters, base poses, and coefficients. They used a 3D gait database to determine base poses constrained by the sum of squared segment lengths. However, the constraint was weak and could not fully represent human poses. Wang et al.[20] advanced this method and constrained the ratios of eight body segments. However, their method ignored the variations in body segment ratios between individuals.

Wandt et al.[23] also used a gait database and used principal component analysis (PCA) of the 3D gait data to extract eigenvectors. They represented a 3D pose as a linear combination of a set of eigenvectors. Using eigenvectors from PCA as base poses, segment lengths could be estimated. They simultaneously optimized camera position continuity and the sum of variances of segment lengths for the entire video frame.

These pose estimation algorithms require joint points in all frames of a video sequence. Practically, it is time consuming to manually mark the joint centers in every frame. In this study, we reconstructed the 3D human pose only for selected gait event frames using frame specific principal components. The gait events were selected to represent specific gait phases such as heel-strike and toe-off. The human poses between the gait events were estimated by interpolating the discrete poses at gait event frames.

In this study, we decomposed camera parameters into a camera projection matrix and a transformation matrix for the model, which was calculated as a combined matrix in previous studies.[20,23] Previously, the absolute positions of a human model could not be calculated because the human model was fixed at the origin, and the camera position was moved.[20,23] However, the camera position is fixed in most video surveillance applications, and the pedestrian moves. As a result, it is important to calculate pedestrian absolute position in order to calculate gait parameters such as step length. We assumed that the camera parameters are known from calibration images and fixed camera intrinsic and extrinsic parameters to increase accuracy in estimating a human pose. Previous studies could not calculate limb length scale because of the lack of camera calibration information. We could calculate absolute limb lengths and tested the validity of limb length estimation.

The effect of camera view angle was evaluated due to reports that the accuracy of recognition is lower in the frontal view compared to the lateral view.[18,28] In this study, pose reconstruction accuracy was analyzed for camera elevation and azimuth angles, and accuracy was improved by using a gait phase-specific PCA method.

Fig. 1 Motion capture data were obtained during walking (left). Three-dimensional anatomical joint positions were calculated and re-projected onto video frames (right)

3. Method

3.1 Data Acquisition

Thirty male subjects (height 171.8±4.7 cm, weight 66.7±6.0 kg) volunteered for this study. We obtained gait data from the subjects at their self-selected walking speed using a motion capture system with nine cameras (MX-T10, Vicon Motion Systems, Oxford, UK). Forty-one reflective markers were attached to subjects according to the plug-in-gait marker set typically used in the Vicon motion capture system, as shown in Fig. 1. We attached three additional markers on the top of the head and one at each toe. Participants were asked to practice walking on the walkway for five minutes. One gait trial was collected from each subject.

Three-dimensional marker trajectories were recorded at 100 Hz. Anatomical joint center 3D trajectories were calculated from the trajectories of the reflective skin markers and subject segment lengths using Vicon Nexus software (ver. 2.5, Vicon Motion Systems, Oxford, UK). We created a stick figure model from 17 points (12 anatomical joint centers, head top, heels, and toes), as shown in Fig. 2. The joints included the left and right shoulders, elbows, wrists, hips, knees, and ankles.

We obtained video sequences of walking from three different views simultaneously using a motion capture system with CMOS cameras (one Canon 60D and two Canon 7D cameras) at a shutter speed of 25 frames per second. Cameras were calibrated using images of a checkerboard to calculate their intrinsic and extrinsic parameters.

We created a virtual camera with elevation and azimuth angles set around the volume of the motion trajectory. The virtual camera projected

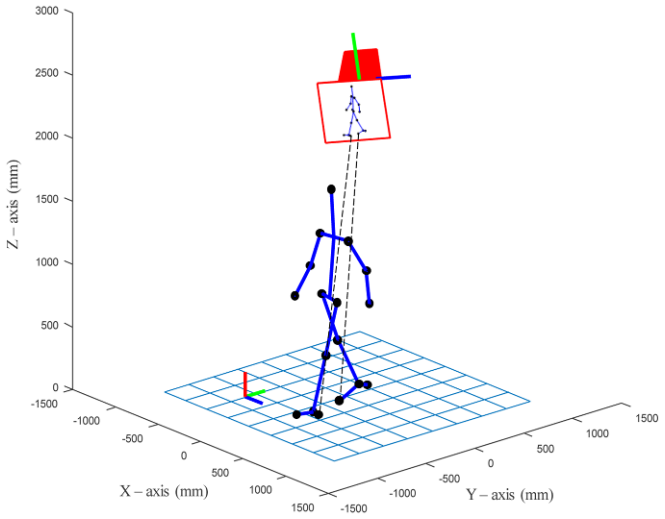

Fig. 2 The three-dimensional stick figure model was made using 17 points (12 joint centers, top of the head, heels, and toes) utilizing subject motion capture data

the joint centers into a two-dimensional plane similar to CMOS cameras. The video sequences obtained with real CMOS cameras were used to validate the virtual camera. The joint centers were projected to the plane of a virtual camera and were used to draw a two-dimensional stick figure.

3.2 Motion normalization and principal components analysis

The walking progression line was aligned to the y-axis. The mid-point between the two hip centers was translated and fixed at the origin. One gait cycle from heel-strike to heel-strike was identified and cropped from the motion capture data for all walking trials. Eight different gait events in the gait cycle (heel-strike, toe-off, early-mid-stance, and late mid-stance of the left and right legs) were manually identified for all gait trials to resample the gait data matching the number of frames between gait events, resulting in 127 frames per gait cycle.

A pose vector (51x1) was composed of the 3D positions of 17 points for each frame. One gait trial had 127 pose vectors. All pose vectors from the gait trials of 30 subjects created a 51 × 3,810 matrix. The PCA was applied to calculate the mean pose and principal components from the pose for the full gait cycle (FGC) data, as performed in previous studies.[23] This approach is referred to as FGC-PCA in the text below.

The pose vectors from 30 percent of the frames of a gait cycle around a gait event (51 × 38 matrix) were extracted and concatenated with those from all gait trials, resulting in a 51 × 1,140 matrix. The PCA was applied to calculate the gait-phase-specific (GPS) mean pose and principal components. There were eight sets of GPS-PCA-based mean pose and principal components for the gait events: heel-strike, toe-off, early-mid-stance, and late mid-stance for the left and right legs.

3.3 Three-dimensional pose reconstruction algorithm

A human pose in a frame is represented as a vector, $P_{3D} \in \mathbb{R}^{51\times1}$, by three-dimensional coordinates of 17 points. The pose vector at the origin is expressed as a linear combination of the mean pose (Q_0) and principal components ($Q_{(i)}$'s) from PCA. We used 25 principal components, as shown below,

$$P_{3D} = Q_0 + \Sigma_{i=1}^{25} \theta_{(i)} Q_{(i)} \quad (1)$$

where $\theta_{(i)}$ is the weight for the i-th principal component, $Q_{(i)}$.

The pose matrix is reshaped to represent homogeneous coordinates of the 17 points, $P'_{3D} \in \mathbb{R}^{4\times17}$. The reshaped pose matrix is transformed by $T \in \mathbb{R}^{4\times4}$ and projected to the image plane of a camera by $M \in \mathbb{R}^{3\times4}$ as follows,

$$(P_{2D})'_{prj} = MTP'_{3D} \quad (2)$$

where $(P_{2D})'_{prj}$ represents the homogeneous coordinate of $(P_{2D})_{prj}$.

The transformation matrix, T, has six variables to be determined, and the camera projection matrix, M, is pre-determined assuming that the camera is calibrated and its pose is known relative to the ground.

During walking, at least one foot is on the ground.[29] If a heel or toe point touches the ground, we can calculate its absolute position in 3D space by calculating the intersection between the line from the camera to the image point and the ground, as illustrated in Fig. 2. The absolute position of the heel and/or toe can be used to estimate the absolute position of the human model.

There are two steps to estimate the transformation matrix, T, and the weight vector, $\Theta = [1, \theta_{(1)}, \ldots, \theta_{(25)}]$. First, we estimated the initial transformation matrix of the human model using the absolute position of the heel and/or toe by minimizing the following object function. Θ is set to [1, 0, …, 0] to use only the mean pose in the beginning as follows,

$$\min_{T} \{ \Sigma_j^{17} \left\| (P_{2D}^j)_{prj} - (P_{2D}^j)_{image} \right\|^3 + \Sigma_n (\gamma \left\| (P_{3D}^{foot})_{abs} - (P_{3D}^{foot})_{model} \right\|)^3 \} \quad (3)$$

where $(P_{2D}^j)_{prj}$ is the i-th joint center projected to the camera image plane, $(P_{2D}^j)_{image}$ is the j-th joint center marked in the video frame, $(P_{3D}^{foot})_{abs}$ is the absolute position of the heel and/or toe point, and $(P_{3D}^{foot})_{model}$ is the 3D position of the matching heel and/or toe point. Here, n represents the number of heel and toe points, and γ is set to 0.2/n, representing the weight to balance the pixel and 3D distance (mm) metrics.

Thereafter, the following optimization routine and the previous optimization routine are executed alternately.

$$\min_{\theta} \{ \Sigma_j^{17} \left\| (P_{2D}^j)_{prj} - (P_{2D}^j)_{image} \right\|^3 + \Sigma_n (\gamma \left\| (P_{3D}^{foot})_{abs} - (P_{3D}^{foot})_{model} \right\|)^3 \} \quad (4)$$

These two steps are iterated until the two object functions converge at a stopping condition. Fig. 3 shows the schematic diagram of reconstructing 3D poses for a full gait cycle.

3.4 Joint kinematics interpolation

The length of each segment was calculated as the average of values in the reconstructed poses in the gait event frames. Among the 17 points representing the 3D pose of a human stick figure model, the center of the two hip joints was used as the root in our model hierarchy. The positions of the root in the gait event frames were interpolated to estimate the root positions in the intermediate frames using the 3D Bezier interpolation method.[30]

Then, the coordinate systems of all segments were determined at the

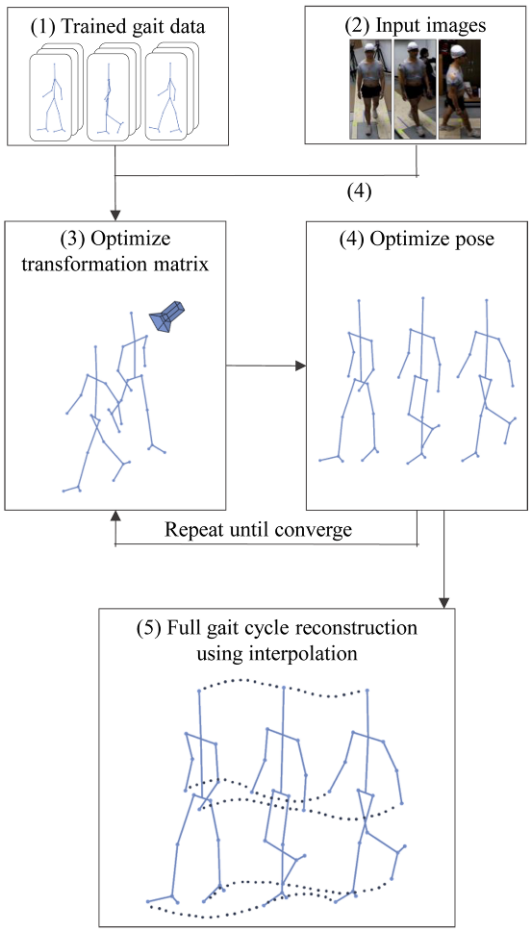

Fig. 3 Schematic diagram. (1) PCA using gait data to generate the mean pose and principal components. (2) Input of a video sequence. (3) Estimation of a transformation matrix of the model to determine the absolute position relative to the camera position. (4) Calculation of weights for principal components to determine the pose. Steps (3) and (4) are repeated alternately to minimize the reprojection error of joint centers. (5) Interpolation of the poses at gait events to reconstruct poses for the full gait cycle

joint points from the positions of the 17 points in each event frame of the gait according to a previous study.[31] We used quaternion representation for interpolating the human motion.[32] Quaternion representations of the 3D rotation of distal segments with respect to proximal segments were calculated between two adjacent segments. The quaternions between gait event frames were interpolated using the Slerp spherical linear interpolation method.[32] The angular displacement in each joint was calculated for the full gait cycle using the interpolated poses.

3.5 Accuracy of pose estimation during a gait cycle

The accuracy of estimating the 3D locations of the 17 body points was quantified as the mean 3D Euclidean distance between the reconstructed points and the measured points from the motion capture system for the eight gait event frames. This pose reconstruction error was calculated repeatedly by changing the camera elevation angle from 0 to 60 degrees at intervals of 15 degrees and the azimuth angle from

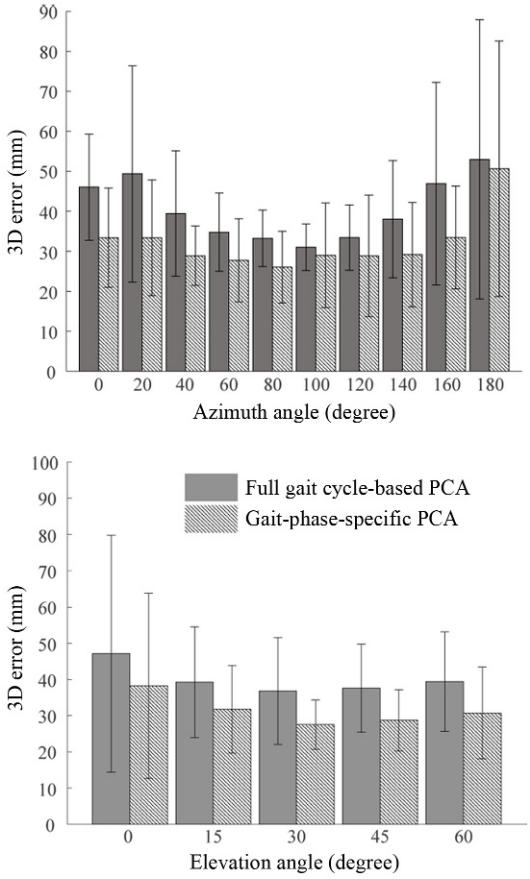

Fig. 4 Influence of camera azimuth angle and elevation angle on the mean 3D position error of the 17 body points for the full gait cycle-based PCA method and gait phase-specific PCA method

0 (front) to 180 degrees (back) at intervals of 20 degrees.

The association between the estimated and measured segment lengths in the eight gait event frames was quantified using a linear mixed effect model with the subjects as a random effect for each body segment including the upper and lower arms and upper and lower legs.

The accuracy of estimating joint angles was quantified as the root mean square (RMS) error over a gait cycle between the interpolated pose and the measured pose from the motion capture system along the three rotational directions for the shoulder, elbow, hip, and knee joints.

The effect of using the locations of the calculated 3D heel and toe points compared to using their true locations on pose estimation and interpolation was determined as the mean 3D Euclidean distance error in each frame of the gait cycle.

4. Experimental Results

4.1 The influence of camera angle on 3D error

Fig. 4 shows the mean position errors of the 17 body points of the reconstructed model in gait event frames with respect to the positions calculated from the motion capture data. The mean position errors were as low as 26 mm at an azimuth angle of 80 degrees in the GPS-PCA method. The mean marker position errors obtained from the GPS-PCA method were lower than those from the FGC-PCA technique at all

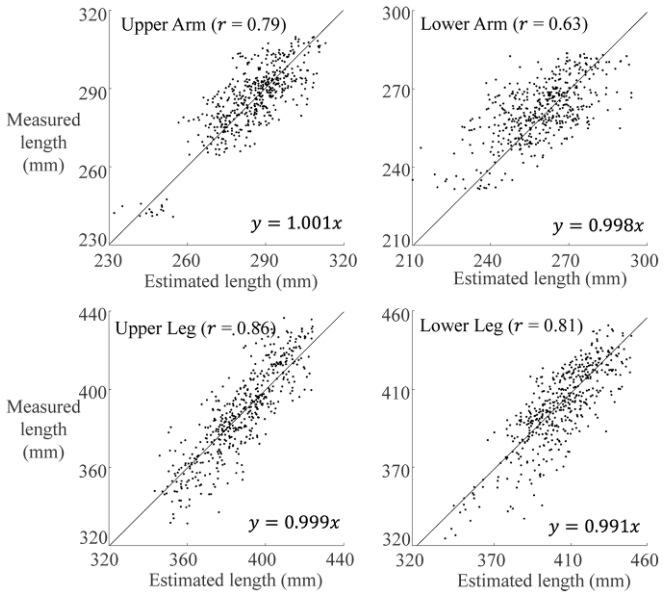

Fig. 5 Segment lengths estimated from the reconstructed pose in the gait event frames

azimuth angles.

The mean position error was higher in the low elevation angles and as low as 28 mm when the elevation angle was 30 degrees in the GPS-PCA method. The error was lower using the GPS-PCA technique compared to FGC-PCA for all elevation angles.

The error of reconstructed 3D poses was highest when the camera was located in the front or back of a person in both the GPS-PCA and FGC-PCA methods. This could be caused by the larger number of candidate poses for each specific gait pose in the front and back views compared to the lateral view. However, it should be noted that the accuracy of the pose reconstructed with the GPS-PCA technique was less affected by azimuth angle except at 180 degrees. The GPS-PCA approach uses the information of the gait phase for the target frame and estimates the weight of principal components calculated from the poses near that gait phase in the database, which would increase the pose estimation accuracy.

4.2 Estimation of segment length

The associations between the estimated segment length in the eight gait event frames and the measured segment length were calculated for the upper arm, lower arm, upper leg, and lower leg, as shown in Fig. 5. The slopes of the regression lines were between 0.991 and 1.001 for the four segments. The correlation coefficients of the upper arm, lower arm, upper leg, and lower leg were 0.79, 0.63, 0.86, and 0.81, respectively. The coefficients of the lower limbs were higher than those of the upper limbs, which should be affected by our objective function, which uses the absolute foot position in estimating the pose.

4.3 Gait interpolation

A full gait cycle was interpolated using nine gait event frames from the left heel strike to the next left heel strike for 30 subjects. Nine gait event frames were calculated using the GPS-PCA method. The results for each subject were calculated at an elevation angle of 45 degrees and an azimuth angle of 90 degrees (lateral view). The mean position error of the 17 body points varied during the gait cycle, as shown in Fig. 6.

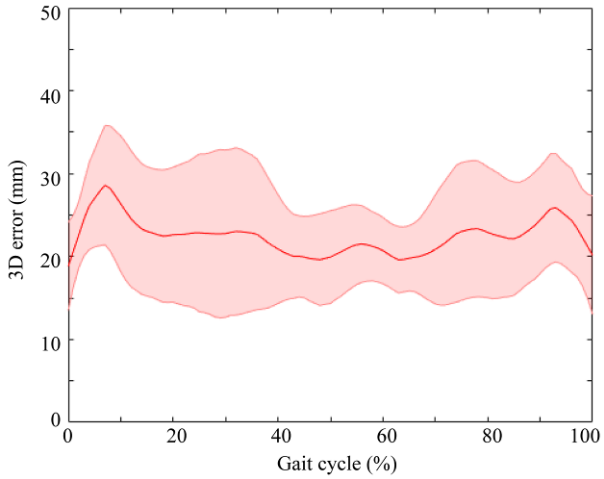

Fig. 6 Mean position error of the 17 body points when the motion was interpolated from the poses in the gait event frames

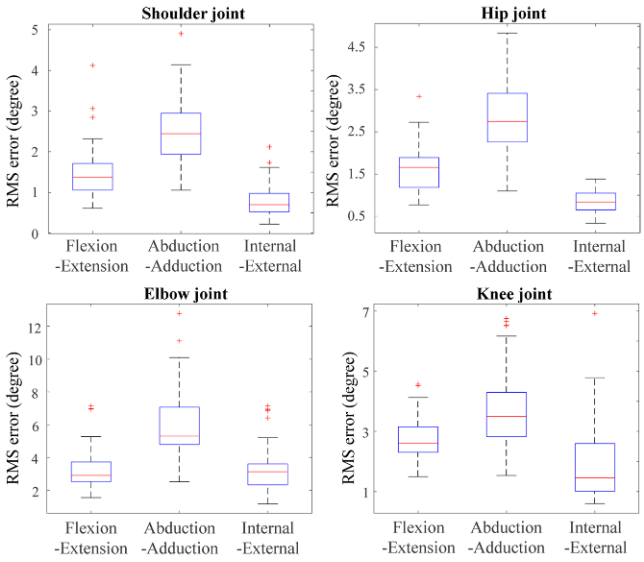

Fig. 7 RMS errors of the estimated joint angles in the shoulder, elbow, hip, and knee joints during a gait cycle

4.4 Root mean square error of the joint angles

The joint angles were quantified along the flexion-extension (FE), abduction-adduction (AA), and internal-external (IE) rotational directions in each joint. The root mean square (RMS) errors of the joint angles were calculated in the shoulder, elbow, hip, and knee.

The mean (SD) values of the RMS error for shoulder joint angle were 1.45 (0.60), 2.49 (0.81), and 0.80 (0.39) degrees for the FE, AA, and IE rotation angles, respectively (Fig. 7). The mean (SD) values of RMS errors for the elbow joint angle were 3.22 (1.21), 5.90 (1.96), and 3.31 (1.35), respectively. The accuracy of the elbow joint angle was lower than that of the other joints because the accuracy of wrist point estimation was lower than that of the lower body points. Overall, the AA rotational angle was less accurate than the FE and IE angles.

5. Conclusions

This paper proposed a method for 3D pose estimation during gait from a single camera video sequence. The PCA was applied to the gait data from 30 subjects to calculate mean pose and principal components. Three-dimensional poses were estimated for the gait event frames in simulated video sequences using FGC-PCA and GPS-PCA. Unlike the FGC-PCA method, the GPS-PCA method uses the gait phase information of the pedestrian in the target image frame. The principal components obtained from the poses in the database around the phase of the target frame could predict the target pose more accurately.

We analyzed the effect of camera view angle on pose reconstruction accuracy. The 3D pose reconstruction from the front and back views was less accurate than that from the lateral camera view. Using a specific gait phase, the accuracy of pose reconstruction increased overall and became less sensitive to camera angle. The correlation coefficients of the segment lengths of the lower limbs were higher than those of the upper limbs, as the objective function had a term determine the absolute position of the foot in estimating the 3D pose.

In addition, a full gait cycle was reconstructed by interpolating estimated poses from gait event frames. The extracted joint angles of the reconstructed 3D gait were highly correlated with measured values in the motion capture data. The accuracy of the elbow joint angle was lower than that of the other joints because the accuracy of wrist position estimation was lower than that of the lower body points. Overall, the AA rotational angle was less accurate than the FE and IE angles. Because the results of gait interpolation were calculated at an azimuth angle of 90 degrees (lateral view), the accuracy of the AA rotational angle was relatively low.

The limitation of the study is that, unlike most real situations, there was only one person in the field of view for gait parameter analysis. In a real situation, the person we want to analyze could be obscured by others. Therefore, research on reconstructing a 3D pose when a part of the body is occluded in CCTV is needed. The 3D reconstructed human motion can reveal the biometric information of a person and has the potential to be used for identification.

ACKNOWLEDGEMENT

This work was supported by the Basic Science Research Program through the NRF (NRF-2017R1A2B2010763) and Projects for Research and Development of Police Science and Technology through CRDPST and KNPA (PA-C000001) funded by the Ministry of Science and ICT of Republic of Korea. It was also supported by the Chung-Ang University Graduate Research Scholarship in 2016.

REFERENCES

1. Jain, A. K., Ross, A., and Prabhakar, S., "An Introduction to Biometric Recognition," IEEE Transactions on Circuits and Systems for Video Technology, Vol. 14, No. 1, pp. 4-20, 2004.
2. Purevsuren, T., Kim, K., Nha, K. W., and Kim, Y. H. "Evaluation of Compressive and Shear Joint Forces on Medial and Lateral Compartments in Knee Joint during Walking Before and after Medial Open-Wedge High Tibial Osteotomy," International Journal of Precision Engineering and Manufacturing, Vol. 17, No. 10, pp. 1365-1370, 2016.
3. Ko, C. Y., Ko, J., Kim, H. J., and Lim, D., "New Wearable Exoskeleton for Gait Rehabilitation Assistance Integrated with Mobility System," International Journal of Precision Engineering and Manufacturing, Vol. 17, No. 7, pp. 957-964, 2016.
4. Jeong, J. Y. and Shin, C. S., "The Effect of Gender and Foot Landing Type on Lower Extremity Biomechanics during Single-Leg Landing," Journal of the Korean Society for Precision Enginering, Vol. 35, No. 1, pp. 33-39, 2018.
5. Kim, J. W., Kwon, Y. R., and Eom, G. M., "Analysis of Dynamic Balance Against Perturbation in Young and Elderly Subjects," Journal of the Korean Society for Precision Enginering, Vol. 35, No. 1, pp. 47-51, 2018.
6. Sarkar, S., Phillips, P. J., Liu, Z., Vega, I. R., Grother, P., and Bowyer, K. W., "The Humanid Gait Challenge Problem: Data Sets, Performance, and Analysis," IEEE Transactions on Pattern Analysis and Machine Intelligence, Vol. 27, No. 2, pp. 162-177, 2005.
7. Wang, L., Tan, T., Ning, H., and Hu, W., "Silhouette Analysis-Based Gait Recognition for Human Identification," IEEE Transactions on Pattern Analysis and Machine Intelligence, Vol. 25, No. 12, pp. 1505-1518, 2003.
8. Lee, L. and Grimson, W. E. L., "Gait Analysis for Recognition and Classification," Proc. of 5th IEEE International Conference on Automatic Face and Gesture Recognition, pp. 155-162, 2002.
9. Kale, A., Sundaresan, A., Rajagopalan, A., Cuntoor, N. P., Roy-Chowdhury, A. K., et al., "Identification of Humans Using Gait," IEEE Transactions on Image Processing, Vol. 13, No. 9, pp. 1163-1173, 2004.
10. Collins, R. T., Gross, R., and Shi, J., "Silhouette-Based Human Identification from Body Shape and Gait," Proc. of 5th IEEE International Conference on Automatic Face and Gesture Recognition, pp. 366-371, 2002.
11. Wang, L., Tan, T., Hu, W., and Ning, H., "Automatic Gait Recognition Based on Statistical Shape Analysis," IEEE Transactions on Image Processing, Vol. 12, No. 9, pp. 1120-1131, 2003.
12. Liu, Z. and Sarkar, S., "Simplest Representation Yet for Gait Recognition: Averaged Silhouette," Proc. of 17th International Conference on Pattern Recognition, pp. 211-214, 2004.
13. Han, J. and Bhanu, B., "Statistical Feature Fusion for Gait-Based Human Recognition," Proc. of IEEE Computer Society Conference on Computer Vision and Pattern Recognition, pp. 842-847, 2004.
14. Cunado, D., Nixon, M. S., and Carter, J. N., "Automatic Extraction and Description of Human Gait Models for Recognition Purposes," Computer Vision and Image Understanding, Vol. 90, No. 1, pp. 1-

41, 2003.

15. Bobick, A. F. and Johnson, A. Y., "Gait Recognition Using Static, Activity-Specific Parameters," Proc. of IEEE Computer Society Conference on Computer Vision and Pattern Recognition, pp. 423-430, 2001.
16. Tanawongsuwan, R. and Bobick, A., "Gait Recognition from Time-Normalized Joint-Angle Trajectories in the Walking Plane," Proc. of IEEE Computer Society Conference on Computer Vision and Pattern Recognition, pp. 726-731, 2001.
17. Lynnerup, N. and Vedel, J., "Person Identification by Gait Analysis and Photogrammetry," Journal of Forensic Science, Vol. 50, No. 1, pp. JFS2004054-2004057, 2005.
18. Bouchrika, I., Goffredo, M., Carter, J., and Nixon, M., "On Using Gait in Forensic Biometrics," Journal of Forensic Sciences, Vol. 56, No. 4, pp. 882-889, 2011.
19. Simo-Serra, E., Ramisa, A., Alenyà, G., Torras, C., and Moreno-Noguer, F., "Single Image 3D Human Pose Estimation from Noisy Observations," Proc. of IEEE Conference on Computer Vision and Pattern Recognition (CVPR), pp. 2673-2680, 2012.
20. Wang, C., Wang, Y., Lin, Z., Yuille, A. L., and Gao, W., "Robust Estimation of 3D Human Poses from a Single Image," Proc. of the IEEE Conference on Computer Vision and Pattern Recognition, pp. 2361-2368, 2014.
21. Ramakrishna, V., Kanade, T., and Sheikh, Y., "Reconstructing 3D Human Pose from 2D Image Landmarks," Proc. of European Conference on Computer Vision, pp. 573-586, 2012.
22. Chen, Y.-L. and Chai, J., "3D Reconstruction of Human Motion and Skeleton from Uncalibrated Monocular Video," Proc. of Asian Conference on Computer Vision, pp. 71-82, 2009.
23. Wandt, B., Ackermann, H., and Rosenhahn, B., "3D Reconstruction of Human Motion from Monocular Image Sequences," IEEE Transactions on Pattern Analysis and Machine Intelligence, Vol. 38, No. 8, pp. 1505-1516, 2016.
24. Gotardo, P. F. and Martinez, A. M., "Non-Rigid Structure from Motion with Complementary Rank-3 Spaces," Proc. of IEEE Conference on Computer Vision and Pattern Recognition (CVPR), pp. 3065-3072, 2011.
25. Park, H. S., Shiratori, T., Matthews, I., and Sheikh, Y., "3D Reconstruction of a Moving Point from a Series of 2D Projections," Proc. of European Conference on Computer Vision, pp. 158-171, 2010.
26. Kim, C. Y., Hong, J. S., and Chun, K. J., "Validation of Feasibility of Two Depth Sensor-Based Microsoft Kinect Cameras for Human Abduction-Adduction Motion Analysis," International Journal of Precision Engineering and Manufacturing, Vol. 17, No. 9, 1209-1214, 2016.
27. Tomasi, C. and Kanade, T., "Shape and Motion from Image Streams under Orthography: A Factorization Method," International Journal of Computer Vision, Vol. 9, No. 2, pp. 137-154, 1992.
28. Goffredo, M., Carter, J. N., and Nixon, M. S., "Front-View Gait Recognition," Proc. of 2nd IEEE International Conference on Biometrics: Theory, Applications and Systems, pp. 1-6, 2008.
29. Winter, D. A., "Human Balance and Posture Control during Standing and Walking," Gait & Posture, Vol. 3, No. 4, pp. 193-214, 1995.
30. Ge, Q. J. and Ravani, B., "Geometric Construction of Bézier Motions," Journal of Mechanical Design, Vol. 116, No. 3, pp. 749-755, 1994.
31. Meredith, M. and Maddock, S., "Motion Capture File Formats Explained," Department of Computer Science, University of Sheffield, Vol. 211, pp. 241-244, 2001.
32. Shoemake, K., "Animating Rotation with Quaternion Curves," Proc. of the 12th Annual Conference on Computer Graphics and Interactive Techniques, pp. 245-254, 1985.